Progress In Electromagnetics Research M, Vol. 57, 175–183, 2017

Comparison of Time-Domain Finite-Difference, Finite-Integration, and Integral-Equation Methods for Dipole Radiation in Half-Space Environments

Craig Warren[1, *], Silvestar Sesnic[2], Alessio Ventura[3], Lara Pajewski[4], Dragan Poljak[2], and Antonios Giannopoulos[1]

Abstract—In this paper we compare current implementations of commonly used numerical techniques — the Finite-Difference Time-Domain (FDTD) method, the Finite-Integration Technique (FIT), and Time-Domain Integral Equations (TDIE) — to solve the canonical problem of a horizontal dipole antenna radiating over lossless and lossy half-spaces. These types of environment are important starting points for simulating many Ground Penetrating Radar (GPR) applications which operate in the near-field of the antenna, where the interaction among the antenna, the ground, and targets is important. We analysed the simulated current at the centre of the dipole antenna, as well as the electric field at different distances from the centre of the antenna inside the half-space. We observed that the results from the simulations using the FDTD and FIT methods agreed well with each other in all of the environments. Comparisons of the electric field showed that the TDIE technique agreed with the FDTD and FIT methods when observation distances were towards the far-field of the antenna but degraded closer to the antenna. These results provide evidence necessary to develop a hybridisation of current implementations of the FDTD and TDIE methods to capitalise on the strengths of each technique.

1. INTRODUCTION

The problem of calculating the radiated fields from a horizontal electric dipole antenna over a half-space is a classical problem in electromagnetics and is often the starting point for many simulations of Ground Penetrating Radar (GPR). It has been extensively studied, beginning with Sommerfeld in 1909 [26, 27], with further work by [1, 13, 29], and more recently [2, 4, 8, 16, 17, 21, 22]. The aim of this research is to compare solutions to this problem using current implementations of the most commonly used numerical techniques, namely: the Finite-Difference Time-Domain (FDTD) method; the Finite-Integration Technique (FIT); and Time-Domain Integral Equation (TDIE) methods. These methods are all well-established in computational electromagnetics since their inceptions: FDTD in 1966 [32]; FIT in 1977 [31]; and TDIE methods in 1973 [12]. Time-Domain methods are particularly well suited (compared with Frequency-Domain methods) for modelling ultra-wide band (UWB) problems, such as GPR, as a broad range of frequencies can be modelled with a single simulation. It is our intention that this work will provide evidence necessary for future development of a hybridisation of current implementations of the FDTD and TDIE methods to capitalise on the strengths of each technique.

In Section 2 we outline the three modelling methodologies, the software used to implement them, and their strengths and weaknesses. In Section 3 we model a dipole antenna first in free space, and

Received 16 February 2017, Accepted 4 June 2017, Scheduled 18 June 2017

* Corresponding author: Craig Warren (Craig.Warren@ed.ac.uk).

[1] School of Engineering, The University of Edinburgh, The King's Buildings, Edinburgh EH9 3JL, UK. [2] FESB, University of Split, R. Boskovica 32, Split HR-21000, Croatia. [3] Department of Engineering, Roma Tre University, via Vito Volterra 62, Rome 00146, Italy. [4] Department of Information Engineering, Electronics and Telecommunications, Sapienza University of Rome, via Eudossiana 18, Rome 00184, Italy.

then over lossless and lossy half-spaces. Here, we compare and analyse the feed-point current and observations of the radiated electric field at different distances from the antenna.

2. MODELLING METHODOLOGIES

All of the three aforementioned techniques (FDTD, FIT and TDIE) are capable of simulating GPR antennas in lossless and lossy environments; however, each has its own set of strengths and weaknesses.

2.1. Finite-Difference Time-Domain (FDTD) and Finite Integration Technique (FIT)

The FDTD solver used in this research is gprMax, which is open-source software that simulates electromagnetic wave propagation for numerical modelling of GPR, and is available at http://www.gprmax.com. gprMax was originally developed in 1996 [6] when numerical modelling using the FDTD method and, in general, the numerical modelling of GPR were in their infancy. Since then a number of commercial [9, 18] and other freely-available [7, 10] FDTD-based solvers have become available, but gprMax has remained one of the most widely used simulation tools in the GPR community. It has been successfully used for a diverse range of applications in academia and industry [3, 20, 23–25, 28], and has almost 300 citations since 2005 [5].

gprMax has recently been redeveloped in Python with a series of improvements made to existing features as well as the addition of several new advanced modelling features including: an unsplit implementation of higher order perfectly matched layers (PMLs) using a recursive integration approach; diagonally anisotropic materials; dispersive media using multi-pole Debye, Drude or Lorenz expressions; soil modelling using a semi-empirical formulation for dielectric properties and fractals for geometric characteristics; rough surface generation; and the ability to embed complex transducers and targets [30].

The FIT is a spatial discretization scheme to numerically solve electromagnetic field problems and can yield results in both time and spectral domains. It was proposed in 1977 by Thomas Weiland and has been continually developed since then [31]. We used Computer Simulation Technology Microwave Studio software for simulations with the FIT. CST is a well-established commercial software tool available at http://www.cst.com. It features a suite of different solvers that use the FIT, Finite Element Method, Method of Moments, and Transmission-line matrix method. In this study we employed the transient solver, which is a general-purpose time-domain electromagnetic simulator implementing the FIT. The FIT method covers the full frequency range of electromagnetics (from static up to high frequency) and optical applications and is the basis not only for the CST transient solver but also for other commercial simulation tools [11].

The strengths of the FDTD and FIT methods are that they are relatively simple to implement, fully explicit, general, and robust techniques. However, they can suffer from errors due to stair-casing of complex geometrical details and the entire computational domain must be discretised which can require extensive computational resources. Computing power is increasing dramatically and becoming more accessible — multi-core CPUs and gigabytes of RAM are now standard features on desktop and laptop machines, and many businesses and universities now have their own High-Performance Computing (HPC) systems. These computational advances have particularly benefitted numerical techniques, such as FDTD and FIT, that discretise the entire computational domain, and thus larger and more complex scenarios can be investigated.

2.2. Time-Domain Integral Equations (TDIE)

The TDIE approach used in this research is based on an extension to the solution of the free space Hallen integral equation given by Eq. (1) [15].

$$\begin{aligned}&\int_0^L \frac{I\left(x', t-\frac{R_a}{c}\right)}{4\pi R_a}dx' - \int_{-\infty}^{t}\int_0^L r(\theta,\tau)\frac{I\left(x', t-\frac{{R_a}^*}{c}-\tau\right)}{4\pi {R_a}^*}dx'd\tau \\ &= \frac{1}{2Z_0}\int_0^L E_x^{inc}\left(x', t-\frac{|x-x'|}{c}\right)dx' + F_0\left(t-\frac{x}{c}\right) + F_L\left(t-\frac{L-x}{c}\right), \end{aligned} \quad (1)$$

where $I(x',t)$ is the unknown axial current along the wire, E_x^{inc} the incident tangential electric field, c the velocity of light in a vacuum, L the length of the dipole, Z_0 the free-space wave impedance, and t the time variable. $R_a = \sqrt{(x-x')^2+a^2}$ and $R_a{}^* = \sqrt{(x-x')^2+4h^2}$ denote the distances between observation point x and source point x' on the actual and image wires, respectively. a is the radius of the dipole, and h is the height above the ground. Unknown functions F_0 and F_L account for the multiple reflections from the wire ends, and can be determined by assuming zero current at the wire ends. The influence of the ground is taken into account via the reflection coefficient function $r(\theta,t)$ given by (2) [15].

$$r(\theta,t) = K\delta(t) + \frac{4\beta}{1-\beta^2}\frac{e^{-\alpha t}}{t}\sum_{n=1}^{\infty}(-1)^{n+1}nK^nI_n(\alpha t), \tag{2}$$

where

$$K = \frac{1-\beta}{1+\beta}, \quad \beta = \frac{\sqrt{\epsilon_r - \sin^2\theta}}{\epsilon_r\cos\theta}, \quad \alpha = \frac{\sigma}{2\epsilon}, \quad \theta = \tan^{-1}\frac{|x-x'|}{2h},$$

and where $\delta(t)$ is the Dirac impulse, and $I_n(t)$ is the n-th order modified Bessel function of the first kind. Properties of the lower half-space are defined with conductivity σ and permittivity $\epsilon = \epsilon_r\epsilon_0$, where ϵ_0 is the permittivity of a vacuum and ϵ_r is the relative permittivity of the lower half-space.

The space-time Hallen equation is solved numerically via the Galerkin-Bubnov variant of the Indirect Boundary Element Method (GB-IBEM), details of which can be found in [15].

The time domain scheme of the GB-IBEM method has shown some advantages over commonly used point-matching techniques (such as the avoidance of kernel quasi-singularity, faster convergence, and easier incorporation of boundary conditions) and it is applicable to more demanding problems including antenna arrays and to some other forms of integro-differential equations types for various thin wire configurations [15]. Furthermore, the Hallen equation does not consist of any space-time differential operator, shown to be the origin of numerical instabilities [19], which makes the use of GB-IBEM more stable compared to the usual marching-on-in-time schemes applied to the Pocklington integral equation containing both space and time derivatives [19].

A novel formula for the transient field transmitted into a lossy half-space is derived in [14] and given by Eq. (3).

$$E_x^{tr}(r,t) = \frac{\mu_0}{4\pi}\int_{-\infty}^{t}\int_0^L \Gamma_{tr}^{\mathrm{MIT}}(\tau)\frac{\partial I(x',t-R''/\nu-\tau)}{\partial t}\frac{e^{-\frac{1}{\tau_g}\frac{R''}{\nu}}}{R''}dx'd\tau, \tag{3}$$

where ν is the velocity of wave propagation in the lower medium, μ_0 the magnetic permeability of vacuum, and R'' the distance from the dipole antenna to the observation point in the lower medium. The influence of an interface between two media is taken into account via the simplified space-time transmission coefficient arising from the Modified Image Theory (MIT) [15] given by Eq. (4).

$$\Gamma_{tr}^{\mathrm{MIT}}(t) = \frac{\tau_3}{\tau_2}\delta(t) + \frac{1}{\tau_2}\left(2-\frac{\tau_3}{\tau_2}\right)e^{-\frac{t}{\tau_2}}, \tag{4}$$

where

$$\tau_2 = \frac{\epsilon_r+1}{\sigma}\epsilon_0, \quad \tau_3 = \frac{2\epsilon_r\epsilon_0}{\sigma}$$

The corresponding transmitted field is obtained by computing the related field integrals using the boundary element formalism as well.

Integral equation methods are generally better suited for modelling complex antenna geometries, but often require either a complicated Green's function or a significant number of unknowns to be able to model the ground.

3. MODEL OF A DIPOLE ANTENNA

A horizontal dipole antenna radiating over a half-space is one of the simplest configurations that exhibit coupling between an antenna and environment. These effects are important for GPR, and also occur

in other electromagnetic applications such as radar imaging for breast cancer detection. The geometry of the scenario is illustrated in Fig. 1. The dipole was of length $L = 1\,\text{m}$, radius $r = 6.74\,\text{mm}$, and was located horizontally above the interface at height $h = 0.1\,\text{m}$. The half-space had a relative permittivity of $\epsilon_r = 10$, and was tested with lossless and lossy ($\sigma = 1, 10\,\text{mS/m}$) configurations. The antenna was excited by specifying a voltage source with a Gaussian shaped waveform given by (5) in a gap between

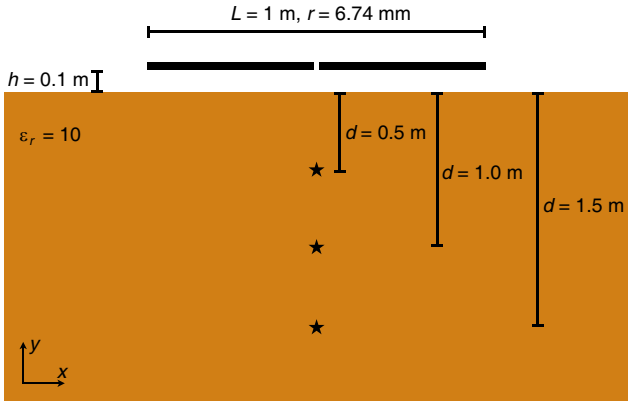

Figure 1. Dipole antenna over a half-space of permittivity $\epsilon_r = 10$, with conductivities $\sigma = 0, 1, 10\,\text{mS/m}$ (star symbols indicate observation locations of the electric field).

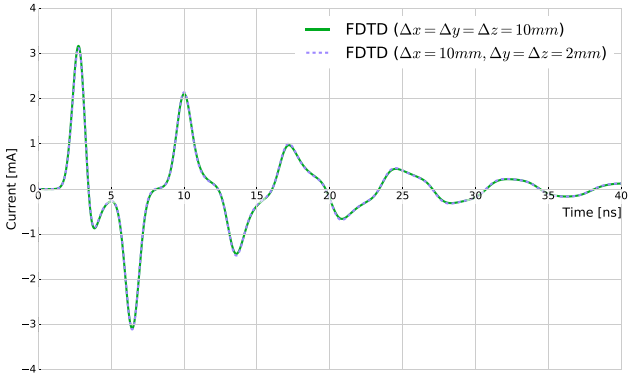

Figure 2. Comparison of different spatial discretisations for FDTD simulation of the current from a dipole in free space.

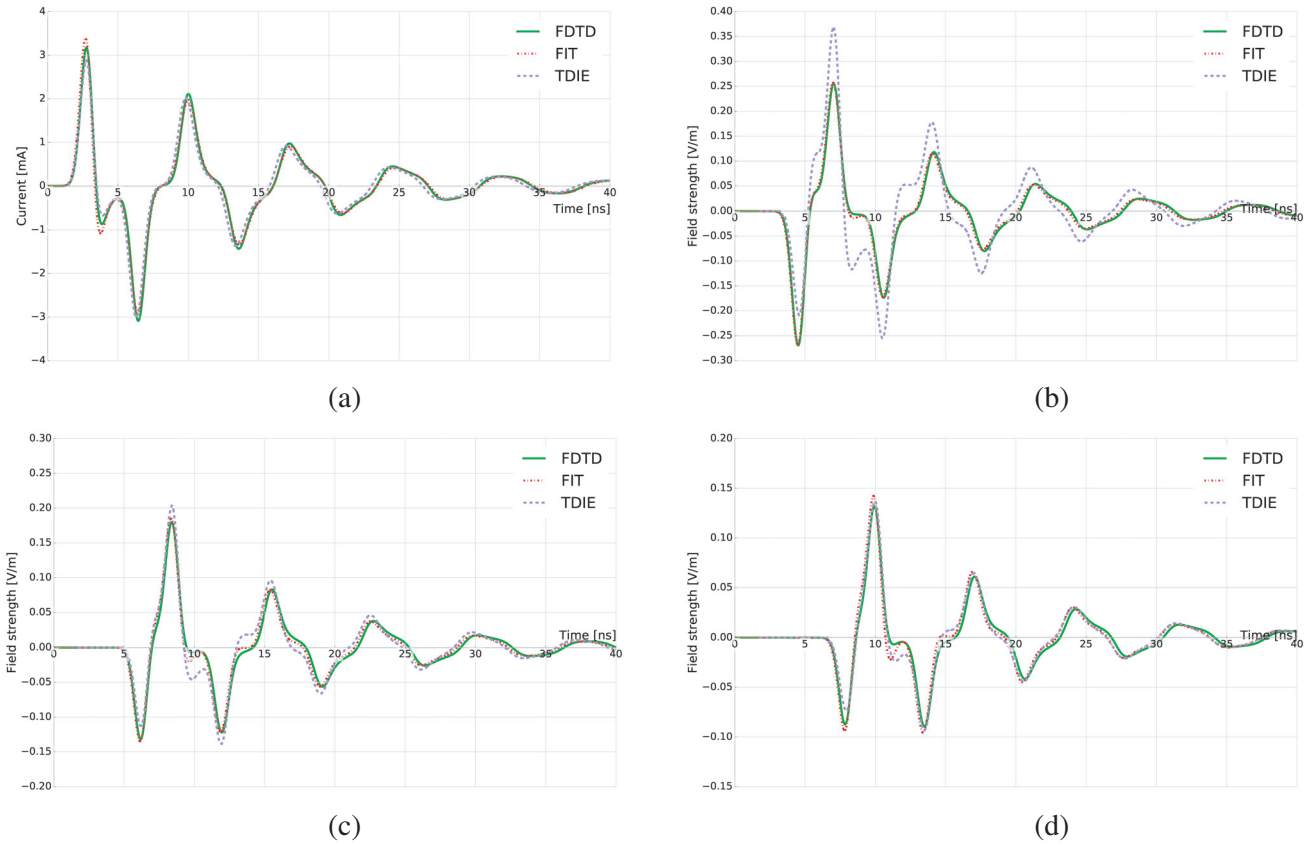

Figure 3. Simulated current and electric field from a dipole in free space. (a) I_x at centre of dipole, (b) E_x at $d = 0.5\,\text{m}$ from centre of dipole, (c) E_x at $d = 1.0\,\text{m}$ from centre of dipole, (d) E_x at $d = 1.5\,\text{m}$ from centre of dipole.

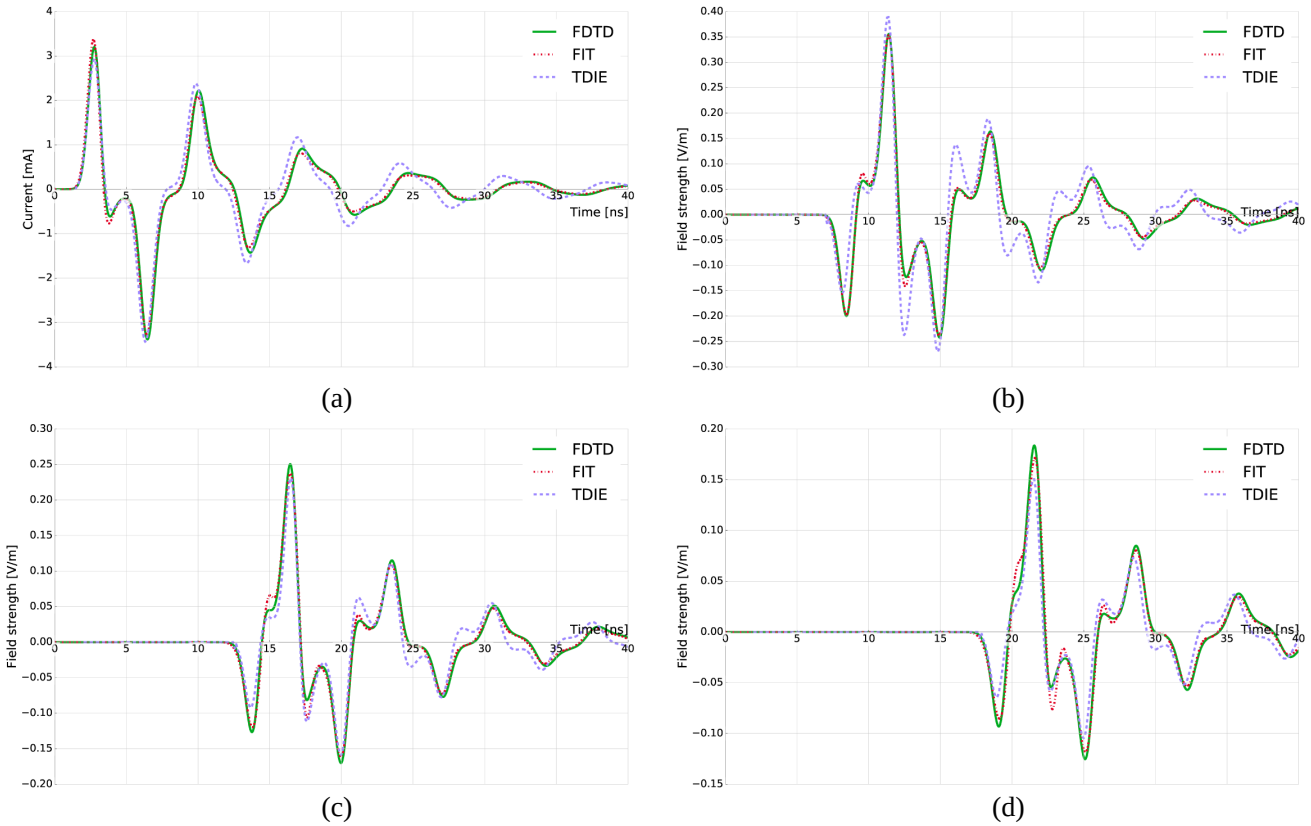

Figure 4. Simulated current and electric field from a dipole at a height of 0.1 m over a lossless half-space of permittivity $\epsilon_r = 10$. (a) I_x at centre of dipole, (b) E_x at $d = 0.5$ m inside half-space, (c) E_x at $d = 1.0$ m inside half-space, (d) E_x at $d = 1.5$ m inside half-space.

the arms of the dipole.

$$V(t) = V_0 \, e^{-g^2(t-t_0)^2}, \tag{5}$$

where $V_0 = 1$ V, $g = 1.5 \times 10^9$, and $t_0 = 1.43 \times 10^{-9}$ s.

To select an appropriate spatial discretisation for the FDTD and FIT simulations, FDTD models with a spatial discretisations of $\Delta x = 10$ mm, $\Delta y = \Delta z = 2$ mm and $\Delta x = \Delta y = \Delta z = 10$ mm were compared. Fig. 2 shows that for both discretisations the simulated waveform of the current at the centre of the antenna (I_x) is almost identical. As such, all the FDTD and FIT models used cubic cells with a spatial discretisation of $\Delta x = \Delta y = \Delta z = 10$ mm as a good compromise between accuracy and computational resources[†]. Therefore, a $10 \times 10 \times 1000$ mm rectangular cuboid was used to represent the cylindrical shape of the dipole antenna, with a 10 mm gap at the centre for a voltage source feed[‡]. The Courant Friedrichs Lewy (CFL) condition was enforced which resulted in a time-step of $\Delta t = 19.26$ ps.

Figure 3 presents the results from the simulations with the antenna in free-space. Although this is not typical of the environment in which a GPR antenna would be used, it provides a basis to begin to evaluate the modelling methodologies. Fig. 3(a) shows the waveform of the current at the centre of the antenna (I_x) which oscillates about the time axis and decays slowly due to the fact that the dipole is not resistively loaded. All of the modelling methodologies agree well in terms of the amplitude and phase of I_x. Figs. 3(b)–3(d) show observations of the electric field (E_x) at distances of 0.5 m, 1.0 m, and 1.5 m perpendicular to the centre of the antenna. At all of the distances the FDTD and FIT results agree well. Furthest from the antenna the TDIE result also agrees with the FDTD and FIT results. As the

[†] Computational resources: FDTD — 450 MB RAM, 160 s runtime (Intel® Core™i7-4790K 4 GHz CPU); FIT — 220 s runtime (Intel® Core™i3-2310M 2.1 GHz CPU); TDIE — 180 s runtime (Intel® Core™i5-4570 3.2 GHz CPU)

[‡] The voltage source used was a hard source, i.e., the voltage prescribes the electric field value at its location.

observation distance is reduced the amplitude of the waveform from the TDIE simulation diverges from the the FDTD and FIT results. This is due to the nature of the approximation of the reflection coefficient in Eq. (2) appearing within the Green's function of time-domain Hallen integral equation (1), and the reflection coefficient in Eq. (4) appearing in the transmitted field integral expression (3). Namely, Eq. (2) stems from a plane wave approximation, while Eq. (4) arises from the MIT, which essentially represents a quasi-static approximation, and both approaches are, strictly speaking, valid in the far-field zone. As a rough estimation, for the frequency domain analysis, in the far-field zone the discrepancy between the approximated reflection coefficient approach and the rigorous Sommerfeld integral representation is up to 10% [15]. In the time-domain, on the other hand, the Sommerfeld integral approach was shown to be unacceptably complex for any practical applications involving thin wire configurations.

Figure 4 presents the same set of observations with the antenna placed over a lossless half-space of permittivity $\epsilon_r = 10$. The FDTD and FIT methods agree well for the current at the centre of the antenna (I_x). After approximately 10 ns there are some slight differences in the amplitude and phase of the waveform from the TDIE method compared to the FDTD and FIT simulations. The same behaviour that was observed in free-space exists in the half-space for the observations of the electric field (E_x), i.e., closer to the antenna there are more significant differences when comparing the waveform from the TDIE method to the FDTD and FIT simulations. These differences are much less apparent as the observation distance becomes further from the antenna.

Figures 5 and 6 present the same set of observations with the antenna placed over lossy half-spaces of permittivity $\epsilon_r = 10$ and conductivities $\sigma = 1\,\text{mS/m}$ and $\sigma = 10\,\text{mS/m}$, respectively. The analyses from the lossless half-space carry over the lossy half-spaces, with a reduction in the amplitudes of the waveforms due to the conductivity.

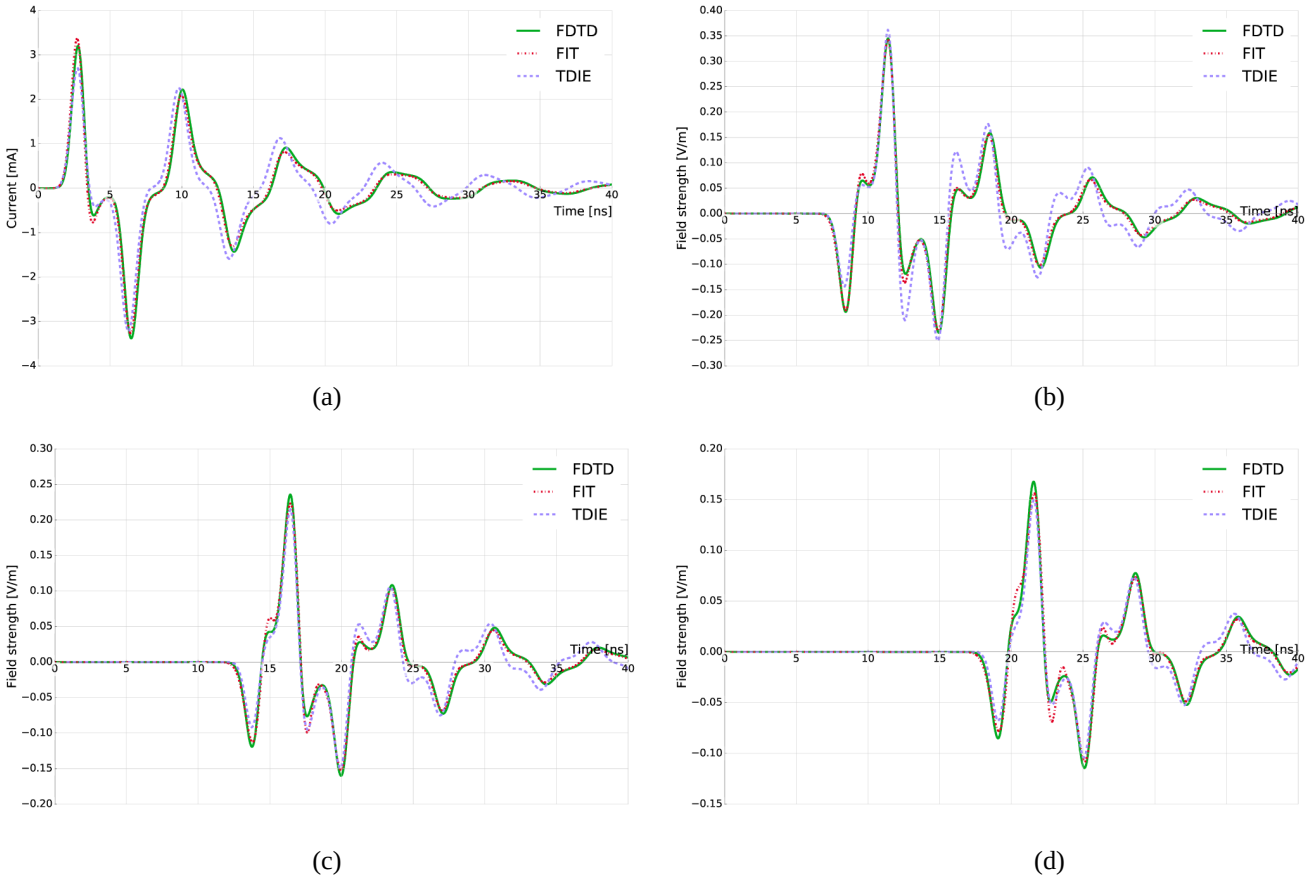

Figure 5. Simulated current and electric field from a dipole at a height of 0.1 m over a lossy half-space of permittivity $\epsilon_r = 10$ and conductivity $\sigma = 1\,\text{mS/m}$. (a) I_x at centre of dipole, (b) E_x at $d = 0.5\,\text{m}$ inside half-space, (c) E_x at $d = 1.0\,\text{m}$ inside half-space, (d) E_x at $d = 1.5\,\text{m}$ inside half-space.

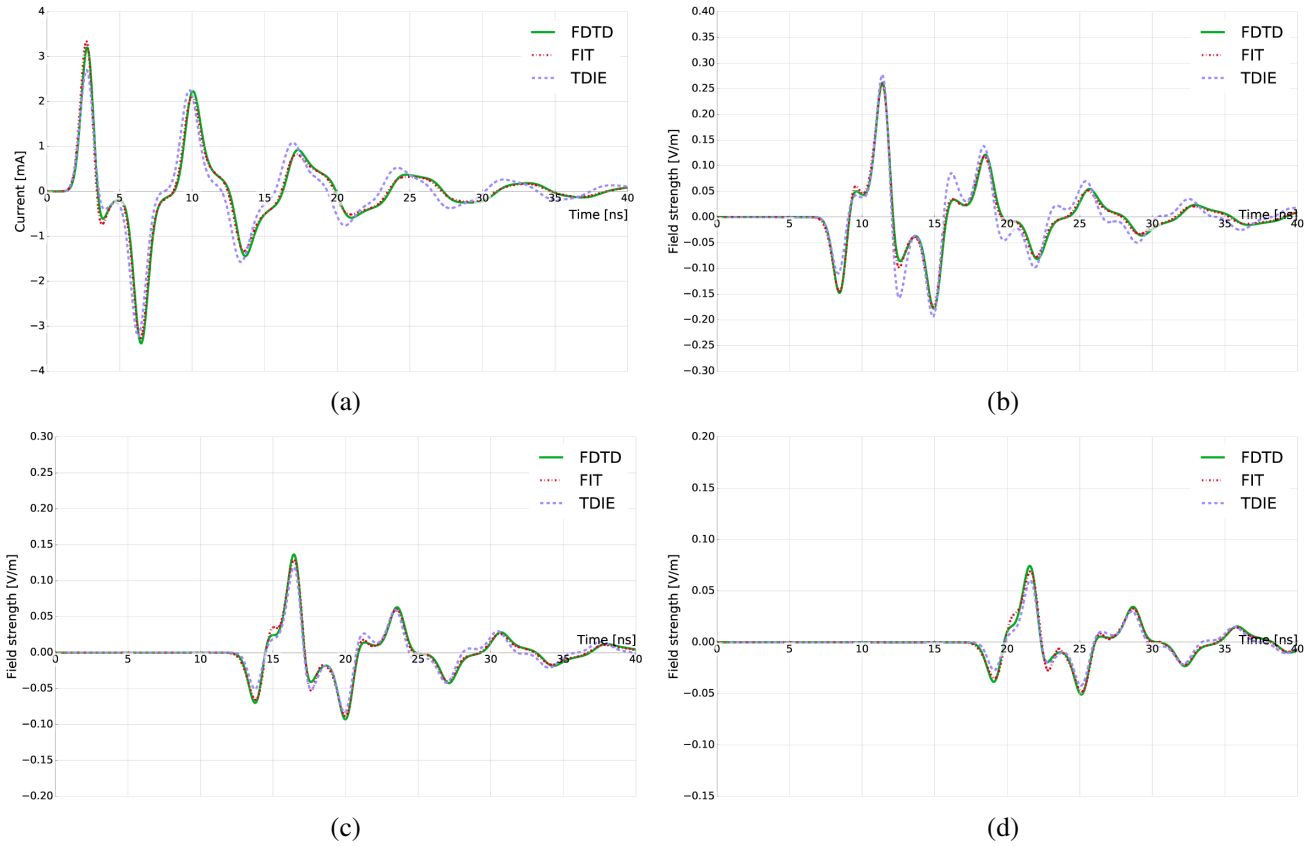

Figure 6. Simulated current and electric field from a dipole at a height of 0.1 m over a lossy half-space of permittivity $\epsilon_r = 10$ and conductivity $\sigma = 10\,\mathrm{mS/m}$. (a) I_x at centre of dipole, (b) E_x at $d = 0.5\,\mathrm{m}$ inside half-space, (c) E_x at $d = 1.0\,\mathrm{m}$ inside half-space, (d) E_x at $d = 1.5\,\mathrm{m}$ inside half-space.

4. CONCLUSION

Three commonly used electromagnetic modelling methods — FDTD, FIT, and TDIE — have been compared by simulating the canonical situation of a horizontal electric dipole antenna radiating over a half-space. Both lossless and lossy half-space environments were modelled. This type of simulation is a useful starting point for examining the performance of GPR. Currently available commercial and open source software were used for the simulations. The current at the centre of the dipole, and the electric field at various distances inside the half-space were observed. All of the results using the FDTD and FIT methods showed good agreement with each other. The TDIE method agreed with the FDTD and FIT methods for the current at the centre of the antenna, and when the observation distance for the electric field was towards the far-field of the antenna. The results demonstrate that these modelling methodologies continue to be suitable for modelling such GPR environments, and provide a basis for establishing a hybridisation of techniques, e.g., FDTD/TDIE. Such a hybridisation could capitalise on the strengths of each method, for example, using the TDIE method to model the antenna coupled with the FDTD method to simulate the ground/structure. This is particularly relevant for the many GPR applications which operate in the near-field of the antenna, where the interaction among the antenna, the ground/structure and targets is important.

ACKNOWLEDGMENT

This work benefited from networking activities carried out within the EU funded COST Action TU1208 "Civil Engineering Applications of Ground Penetrating Radar."

REFERENCES

1. Banos, A., Jr. and J. P. Wesley, "The horizontal electric dipole in a conducting half-space," Scripps Institution of Oceanography, 1953.
2. Bretones, A. R. and A. G. Tijhuis, "Transient excitation of a straight thin wire segment over an interface between two dielectric half spaces," *Radio Science*, Vol. 30, No. 6, 1723–1738, 1995.
3. Cassidy, N. J. and T. M. Millington, "The application of finite-difference time-domain modelling for the assessment of GPR in magnetically lossy materials," *Journal of Applied Geophysics*, Vol. 67, No. 4, 296–308, 2009.
4. Chen, H. T., J.-X. Luo, and D.-K. Zhang, "An analytic formula of the current distribution for the vlf horizontal wire antenna above lossy half-space," *Progress In Electromagnetics Research Letters*, Vol. 1, 149–158, 2008.
5. Elsevier, Scopus, the largest abstract and citation database of peer-reviewed literature, [online], http://www.scopus.com, Mar. 24, 2017.
6. Giannopoulos, A., "Modelling ground penetrating radar by gprMax," *Construction and Building Materials*, Vol. 19, No. 10, 755–762, 2005.
7. Gwangju Institute of Science and Technology, GMES — Gist Maxwell's equations solver, [online], http://sourceforge.net/projects/gmes/, Mar. 24, 2017.
8. Liu, L. and S. A. Arcone, "Propagation of radar pulses from a horizontal dipole in variable dielectric ground: A numerical approach," *Subsurface Sensing Technologies and Applications*, Vol. 6, No. 1, 5–24, 2005.
9. Lumerical Solutions, Inc., FDTD solutions, [online], https://www.lumerical.com/tcad-products/fdtd/, Mar. 24, 2017.
10. Massachusetts Institute of Technology, Meep — Mit electromagnetic equation propagation, [online], http://ab-initio.mit.edu/wiki/index.php/Meep, Mar. 24, 2017.
11. Mentor Graphics, Electromagnetic simulation solutions, [online], https://www.mentor.com/pcb-/nimbic/, Mar. 24, 2017.
12. Miller, E. K., A. J. Poggio, and G. J. Burke, "An integro-differential equation technique for the time domain analysis of thin wire structures. I. The numerical method," *Journal of Computational Physics*, Vol. 12, No. 1, 24–48, 1973.
13. Moore, R. K. and W. E. Blair, "Dipole radiation in a conducting half-space," *Journal of Research of the National Bureau of Standards — D. Radio Propagation*, Vol. 65, No. 6, 547–563, 1961.
14. Poljak, D., S. Sesnic, D. Paric, and K. El Khamlichi Drissi, "Direct time domain modeling of the transient field transmitted in a dielectric half-space for gpr applications," *2015 International Conference on IEEE Electromagnetics in Advanced Applications (ICEAA)*, 345–348, 2015.
15. Poljak, D., *Advanced Modeling in Computational Electromagnetic Compatibility*, John Wiley & Sons, 2007.
16. Poljak, D. and V. Roje, "Time domain calculation of the parameters of thin wire antennas and scatterers in a half-space configuration," *IEE Proceedings — Microwaves, Antennas and Propagation*, Vol. 145, No. 1, 57–63, 1998.
17. Rančić, M. P. and P. D. Rančić, "Horizontal linear antennas above a lossy half-space: A new model for the Sommerfeld's integral kernel," *International Journal of Electronics and Communications (AEU)*, Vol. 65, No. 10, 879–887, 2011.
18. Remcom, Xfdtd em simulation software, [online], http://www.remcom.com/xf7, Mar. 24, 2017.
19. Rynne, B. P. and P. D. Smith, "Stability of time marching algorithms for the electric field integral equation," *Journal of Electromagnetic Waves and Applications*, Vol. 4, No. 12, 1181–1205, 1990.
20. Shangguan, P. and I. L. Al-Qadi, "Calibration of fdtd simulation of GPR signal for Asphalt pavement compaction monitoring," *IEEE Transactions on Geoscience and Remote Sensing*, Vol. 53, No. 3, 1538–1548, 2015.
21. Shoory, A., R. Moini, and S. H. H. Sadeghi, "Direct use of discrete complex image method for evaluating electric field expressions in a lossy half space," *IET Microwaves, Antennas &*

Propagation, Vol. 4, No. 2, 258–268, 2010.

22. Slob, E. and J. Fokkema, "Coupling effects of two electric dipoles on an interface," *Radio Science*, Vol. 37, No. 5, 2002.
23. Slob, E., M. Sato, and G. Olhoeft, "Surface and borehole ground-penetrating-radar developments," *Geophysics*, Vol. 75, No. 5, 75A103–75A120, 2010.
24. Soldovieri, F., J. Hugenschmidt, R. Persico, and G. Leone, "A linear inverse scattering algorithm for realistic GPR applications," *Near Surface Geophysics*, Vol. 5, No. 1, 29–42, 2007.
25. Solla, M., R. Asorey-Cacheda, X. Núñez-Nieto, and B. Conde-Carnero, "Evaluation of historical bridges through recreation of gpr models with the FDTD algorithm," *NDT & E International*, Vol. 77, 19–27, 2016.
26. Sommerfeld, A., "Über die ausbreitung der wellen in der drahtlosen telegraphie," *Annalen der Physik*, Vol. 333, 665–736, 1909.
27. Sommerfeld, A., "Über die ausbreitung der wellen in der drahtlosen telegraphie," *Annalen der Physik*, Vol. 386, No. 25, 1135–1153, 1926.
28. Tran, A. P., F. Andre, and S. Lambot, "Validation of near-field groundpenetrating radar modeling using full-wave inversion for soil moisture estimation," *IEEE Transactions on Geoscience and Remote Sensing*, Vol. 52, No. 9, 5483–5497, 2014.
29. Wait, J. R., "The electromagnetic fields of a horizontal dipole in the presence of a conducting half-space," *Canadian Journal of Physics*, Vol. 39, No. 7, 1017–1028, 1961.
30. Warren, C., A. Giannopoulos, and I. Giannakis, "GPRMAX: Open source software to simulate electromagnetic wave propagation for ground penetrating radar," *Computer Physics Communications*, Vol. 209, 163–170, 2016.
31. Weiland, T., "A discretization model for the solution of Maxwell's equations for six-component fields," *Archiv Elektronik und Uebertragungstechnik*, Vol. 31, 116–120, 1977.
32. Yee, K. S., "Numerical solution of initial boundary value problems involving Maxwell's equations in isotropic media," *IEEE Transactions on Antennas and Propagation*, Vol. 14, No. 3, 302–307, 1966.